Volume 1, No.1, 1984

Journal of the Faculties of
Engineering of Uludağ University

EFFECTS OF GRAVITY ON INTERDENDRITIC FLUID FLOW IN LARGE REMELTED INGOTS

Metin YEREBAKAN*

Department of Mechanical Engineering
Uludağ University, Tezok Campus
Hürriyet, Bursa, Turkey

SUMMARY

This paper presents analytic calculations of the interdendritic fluid-flow in mush zones whose width is small compared to their length, a situation which is caracteristic of large remelted ingots. The flow is found to consist of two main components. The first one is normal to the isotherms which feeds solidification shrinkage and the second one is parallel to the isotherms which is produced by gravity acting on desity differences in the interdendritic liquid. If the isotherms are not exactly parallel, then the gravity induced flow parallel to the isotherms induces a component normal to it. This companent may cause the freckles that occur in remelted ingots when melting conditions are changed.

1. INTRODUCTION

Recently a number of groups have reported calculations of interdendritic fluid flow and macrosegregation in casting ingots (1-6) with the exceptions of the works done by the Cabot Corporation[3] and J.J. Favier[6]. These studies have analysed the solidification of small Sn- % 20 Pb ingots. This is because the calculations required the temperature distribution in the ingots to be known before macrosegregation could be calculated and experimental measurements of temperatures in large ingots are difficult to perform.

The purpose of this paper is to present an approximate analytic calculation of fluid flow in a context appropriate for large remelted ingots. The analytic approach allows a clarer understanding of the flow than is given by the numerical calculations.

2. GOVERNING EOUATIONS

The equations (1-3) below describe the interdendritic fluid flow of a binary alloy in which no diffusion occurs in the solid. The equations can also describe the solidification of a multicomponent alloy

---

* *Yard. Doç. Dr.*

if only one phase is forming. In this case C_L represents the concentration of some species in the liquid and k its partition ratio. These equations were first obtained by Mehrabian et al. (1970) and generalisations have been discussed by others[3-5].

$$\frac{\partial}{\partial t}(\rho_L g_L) - \rho_S \frac{\partial g_L}{\partial t} = -\nabla(\rho_L g_L \underset{\sim}{v}) \tag{1}$$

$$\frac{\partial g_L}{\partial t} = -\left(\frac{1-\beta}{1-k}\right)\frac{g_L}{C_L}\frac{\partial C_L}{\partial T}\left[\frac{\partial T}{\partial t} + \underset{\sim}{V}\nabla T\right] \tag{2}$$

$$\underset{\sim}{V} = \frac{K(g_L)}{\mu}\left[-\nabla P + \rho_L \underset{\sim}{g}\right] \tag{3}$$

In these equations, g_L, $\underset{\sim}{v}$ and P are unknowns, where g_L is the volume fraction liquid, P is the fluid pressure and, $\underset{\sim}{v}$ interdendritic fluid velocity. The other symbols are defined as follows: ρ_L and ρ_S are the liquid and solid densities, β is the solidification shrinkage, k is the partition ratio, C_L is the liquid composition, μ is the viscosity of the liquid, g is the acceleration of gravity, and $K(g_L)$ is the permeability of the dendritic network.

All quantities are taken to be known functuons of temperature; in particular, the assumption that k and ρ_S be constant made in earlier work by Kou et al. (1977) is not required if k and represent the values at the solid-liquid interface.

After the lengthy algebraic manipulation described in appendix equations (1-3) can be rewritten as,

$$\frac{\partial}{\partial t}(\rho_L g_L) - \rho_L \frac{\partial g_L}{\partial t} = -\nabla\cdot(\rho_L g_L \underset{\sim}{\bar{V}}) - \cdot(\rho_L g_L \underset{\sim}{\bar{V}} p) \tag{4}$$

$$\frac{\partial g_L}{\partial t} = -\left(\frac{1-\beta}{1-k}\right)\frac{g_L}{C_L}\frac{\partial C_L}{\partial T}\left[\frac{\partial T}{\partial t} + \underset{\sim}{\bar{V}}\cdot\nabla T\right] \tag{5}$$

$$\underset{\sim}{\bar{V}} = \frac{K(g_L)}{\mu}(-\nabla P) \tag{6}$$

where the new velocity V is related to the old one by,

$$\underset{\sim}{\bar{V}} = \underset{\sim}{V} - \underset{\sim}{V_p} \tag{7}$$

with V_p being a velocity parallel to the isotherms which depends on g_L but not on $\underset{\sim}{V}$ (see appendix 1). $\underset{\sim}{V_p}$ is proportional to the acceleration of gravity.

The only term involving gravity is $[-\nabla\rho_L g_L \underset{\sim}{V_p}(x, y, g_L)]$. Thus the effect of gravity is to drive a flow with velocity $\underset{\sim}{V_p}$, along the isotherms. If the isotherms are not parallel, then this flow induces other flows normal to the isotherms in order to conserve mass.

In general, the mushy zone in large remelted ingots tends to be thin compared to its length, Figure 1 shows liquidus and eutectic for a Waspaloy ingot calculated by Jeanfils et al. (1981). Over most of the ingot, the mushy zone thickness is less than about 20 % of the ingot radius. Furthermore, in materials with light solute elements., macrosegregation tends to develop away from the ingot center, which is where the mushy zone is thickest.

If the mushy zone is long and thin, then derivatives of quantities in directions perpendicular to the isotherms will be large compared with derivatives parallel to isotherms. In the equations (4-6) suppose that

the x-axis is aligned parallel to the isotherms and the y-axis normal to them. Then, if derivatives with respect to x are ignored, the solution $V_x = 0$ satisfies equation (4-6). This entails

$$V_x(y) = \underline{V}_p = \frac{K}{\mu} \left[\rho_L(y) - \rho_L\left(y\left(T_L\right)\right)\right] \tag{8}$$

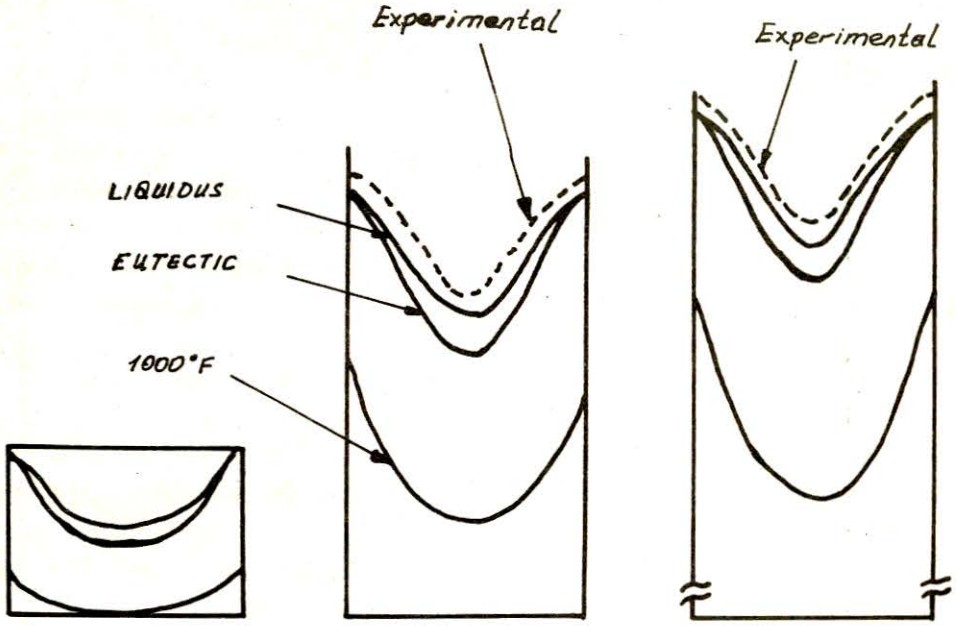

Figure 1 — Comparison of pool profile prediction and experimental pool profiles in a 40 cm diameter "Waspaloy" alloy ingot. The eutectic and the 540°C isotherms are also shown.

With T_L being the liquidus temperature. Although this expression for the velocity parallel to isotherms depends on the unknown g_L via its dependence on K, for practical purposes this is not important. In real remelted ingots, g_L seldom departs much form the value given by the Scheil equation except in small regions; if it did, one would expect composition fluctuations over large parts of ingots, contrary to reports (Ridder et al., 1978, Jeanfils et al., 1981).

A plot of v_x versus temperature at midradius in the mushy zone of the ingot analysed by Jeanfils et al. is shown in Figure 2. Mehrabian et al. (1970) suggested that K was proportional to g_L, an assumption which has been used in most subsequent numerical work. In this case, one can see that the velocity component $\underline{V}_x$ has a shallow maximum nearly midway between the liquidus and eutectic. In this calculation the raio K/g_L^2 has been assumed to be 6×10 m^2, which is the value suggested by Jeanfils et al. (1981).

Piwonka and Flemings (1966) reported measurements of the permeability K of semisolid Al-Cu alloys and found

$$K = \begin{cases} \gamma_1 \, g_L^2 & g_L \leq 0.4 \\ \gamma_2 \, g_L^9 & g_L \geq 0.4 \end{cases} \tag{9}$$

For the dashed curve in Figure 2, the permeability has been assumed to follow (g_L) with the constants γ_1 and γ_2 chosen to be 6×10^{-11} m^2 and 3.6×10^{-8} m^2 to assist comparison with the other data. In reality,

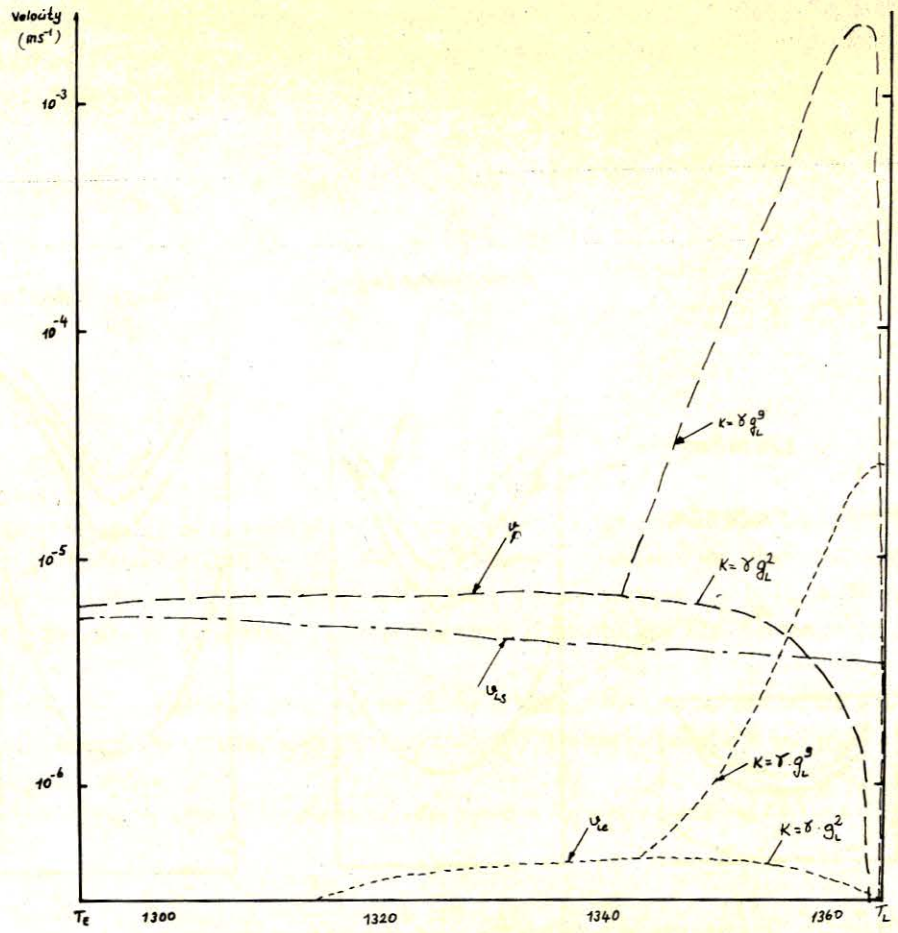

Figure 2 — Interdendritic fluid-flow in a waspalloy ingot.; velocity parallel to isotherms ,: velocity perpendicular to isotherms induced by shrinkage: is velocity perpendicular to isotherms induced by gravity.

both constants would be produced than is observed experimentally. Using this form, V_x has a large peak very close to the liquidus. Orher measurements of permeability over more limited temperature ranges (10) suggest that the measurements of Piwonka and Flemings may have exaggerated the rate of rise of permeability with increasing g_L. If could be noted that there is a maximum in V_x near the liquidus, although not as large as the one shown in Figure 2.

The other component V_y is obtained from (4) and (5) with derivatives with respect to x being set to zero. This reduces (4) and (5) to the system of equations treated by Flemings and Nereo[1] values for V_y are included on Figure 2 for comparison with V_x assuming an isotherm velocity of 10^{-4} m/s (used by Jeanfils et al., 1981, in their casting) in steady-state conditions. It can be stressed that the velocity component V_y induced by solidification shrinkage is independent of gravity. Conversely, the component V_x is independent of the cooling rate and depends only on the force of gravity. Thus, if the isotherms stopped moving for a moment, V_y would fall to zero, but V_x would be unaffected.

3. EFFECTS OF MUSHY ZONE GEOMETRY ON FLOWS

The flow component described by V_x in equation (8) cannot affect segregation directly since it runs parallel to isotherms and only flow normal to them can affect solidification (9). However, if the

isotherms are not parallel, then, in order to conserve mass, the main flow parallel to the isotherms must cause some flow normal to the isotherms. These flows can produce segregation.

If the isotherms are nearly parallel, then under quite general conditions the gravity-induced flow velocity normal to the isotherms is given by (see appandix 2).

$$V_{yg} = \frac{-1}{g_L \rho_L} \int_{y(T_L)}^{y} dy \; \nabla \cdot (\rho_L \; g_L \; V_p) \tag{10}$$

Where y-ax is is normal to the isotherms.

There are three main ways the flow parallel to the interface in a remelted ingot could be bent away from a direction parallel to isotherms. First, the isotherms are usually close together near the mold wall and farther apart at the center. Second, the isotherms are bent towards the horizontal at the mold center. Finally, most remelted ingots are cylindrical and so geometrical factors force some flow normal to isotherms if the flow parallel to them is constant. In the first case, the isotherms might be parallel to the surfaces as;

$$y\ (1+2ax) = \text{constant} \tag{11}$$

in a cartesian coordinate system with x-axis parallel to the eutectic line, as seen in Figure 3 (a). Here a is a small parameter at midradius in one ingot described by Jeanfils et al[9], $a = 0.04\ t_m^{-1}$ where t_m is the mushy zone thickness.

Equation (10) is evaluated in appendix 2 for this case;

$$V_{yg} = 2\ a g_{yx}\ \ J\ (y) \tag{12}$$

where the function J is defined by

$$J = (g_L \rho_L)^{-1} \int_{y(T_L)}^{y} dy\ (\rho_L\ g_L/\mu)[\ \rho_L(y) - \rho_L(-y_{T_L})] \tag{13}$$

Here T_E is eutectic temperature while T_L is liquidus temperature. The solution is accurate to first order in a and the solidification shrinkage. Slow variation of quantities parallel to the liquidus has also been assumed. The calculated results is plotted in figure 2 using value for the waspalloy ingot as described before.

The effects of isotherms curvature can be calculated in a similar way under similar conditions (see appandix 3) to give;

$$V_{yg} = -2\ a\ g_y\ J(y) \tag{14}$$

where isotherms have been chosen to be parallel to the surfaces as shown in Figure 3. b.

$$Y - ax^2 = \text{constant} \tag{15}$$

Because of uncertainty in measuring of dendrite arm spacings in order establish an analytic expression of permeability, the analytic expression have been used.

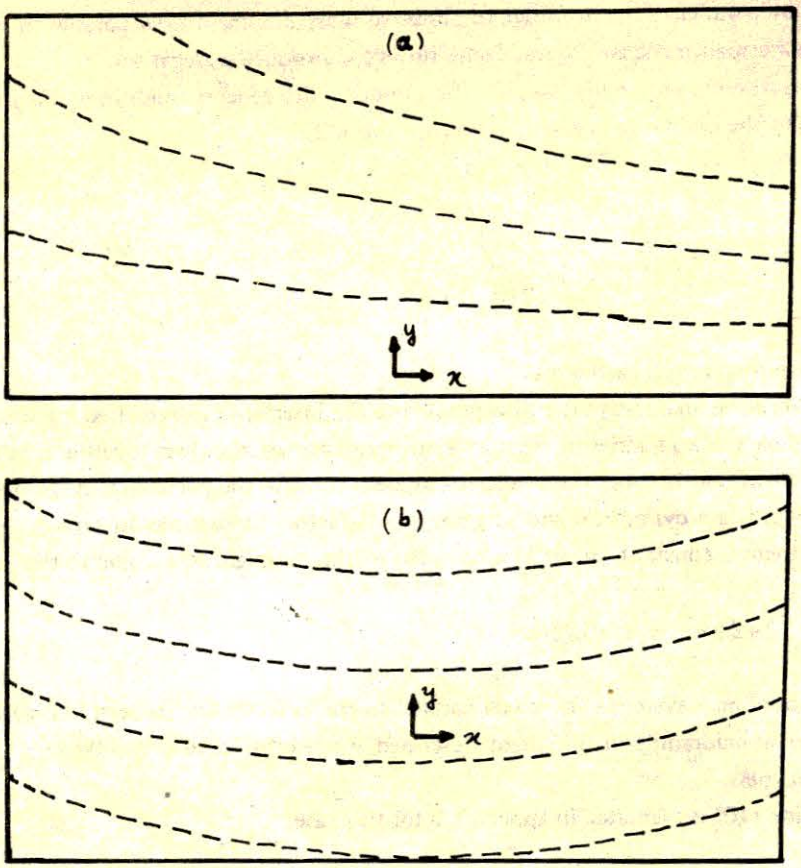

Figure 3 — a. Convergent isotherms $T = T_o\, y\, (1 + 2ax)$
b. Curved isotherms. $T = T_o\, (y - ax^2)$

The Figure 3 shows that the main influences on flow in the ingots are the isotherms and ingot curvature near the center and the flow induced by isotherm convergence farther out. Only beyond midradius there is a gravitydriven component normal to the isotherms. Since the calculations are made under the assumption that quantities vary slowly in the direction parallel to the isotherms, results obtained in the region where the flow is changing rapidly are likely not to be very acurate. This explains why Figure 4 appears to suggest that gravity-driven flow causes not a gain of interdnedritic liquid from the musny zone.

Variable dendrite arm spacings represent a further complication. However this also can be overcome to establish an expression of timedenpendent permeability function given by Yerebakan[11].

Near the edges of the ingot, the dendrite arm spacings and hence the permeability are expected to be less than at the center, because cooling rate is greather apart from the center of an ingot. This will reduce gravity-driven flow at the edge because it is strongly dependent on the permeability. In this region the shrinkage-driven flow will not be affected.

4. THE FORMATION OF MACROSEGREGATES

In the previous sections, it has been shown that the main effect of gravity on interdendritic fluid-flow in large remelted ingots is to produce a flow parallel to the isotherms described by equation 8. This flow cannot by itself produce macrosegregates, but when the isotherm geometry forces it to change, then flows normal to the isotherms are produced macrosegregates.

A comparison of the gravity induced flow shown in Figure 4. with the shrinkage-induced flow in Figure 2. shows that under the conditions using which this ingot was made, the gravity-induced flows are

mostly small compared to the shrinkage-induced ones. Consequently they will not normally produce serious segregation. Finally, the circular cross-section of the ingot affects fluid-flow. The relevant expression for the velocity component is obtained in appendix 3.

$$V_{yg} = \frac{-g_x \cos \theta}{r} J_{(y)} \qquad (16)$$

Where θ is the angle between the isotherm normal and the vertical axes and r is radial pasition.

Figure 4 shows the maximum magnitudes of all of these flows plotted as functions of radial position in a Waspalloy ingot.

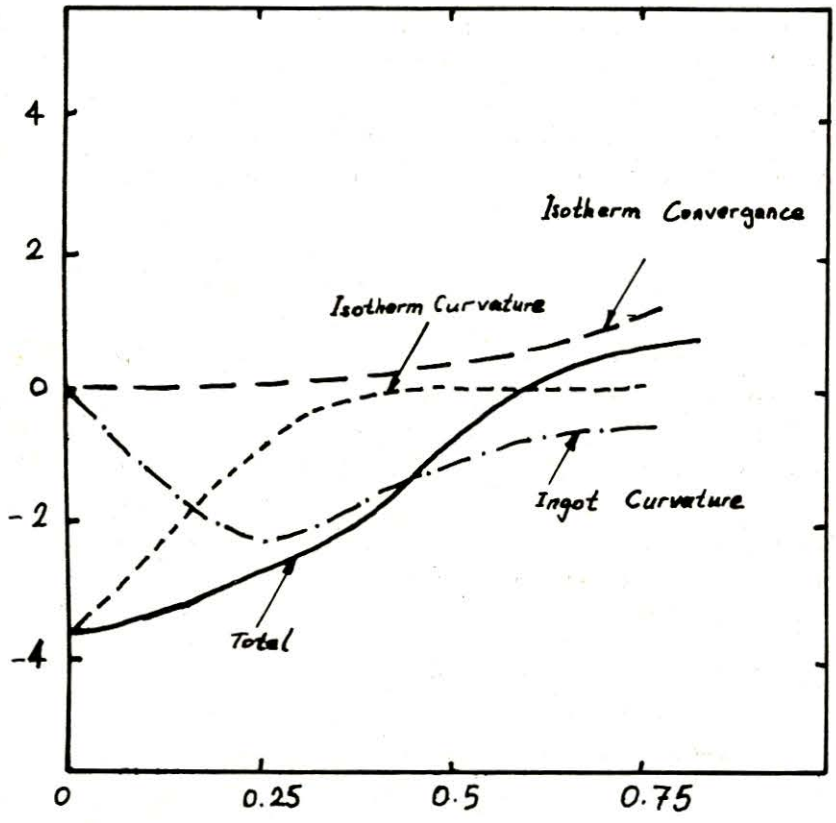

Figure 4 — Magnitude of various contributions to gravity-driven flow normal to isotherms.

No value are given near the mold wall because some of the assumptions underlying the calculation are not justified there.

Although the relative magnitudes of the flows are independent of the exact form of the permeability, the expression given by Mehrabian et al[8] has been used.

This conclussion rests upon the assumption that the temperature in the mushy zone is decreasing smothly. In practice, this may not occur. For example, if the melt rate in an ESR furnace is increased, increased heat may be suplied to the mushy zone. This might stop the upward isotherm movement momentarily. In turn, this would stop fluid-flow induced by shrinkage, leaving only the gravity induced flow which not greatly affected by temperature fluctuations.

Figure 4 shows that, away from the ingot center, this flow goes in the direction of increasing teperature. Thus it is likely that the criterion for the formation of macrosegretages proposed by Mehrabian et al.[2],

$$\frac{V \nabla T}{\partial T / \partial t} < -1 \qquad (17)$$

would be satisfied and freckles would be produced at some position fruther from the ingot center than about one half of the ingot radius. Jeanfils et al. observed freckle formation when the melt rate was increased.

Studies related to ingot casting[4,5,8] suggest that the properties of the mushy zone near the liquidus are important in the formation of A-segregates, which are probably formed by the same mechanism as freckles in remelled ingots. The interpretation of Figure 2 concludes that the gravity induced flow normal to isotherms attains a maximum at the liquidus and the magnitude of the flow is sensitive to the permeability near the liquidus temperature in the semi-solid region. The calculations given in this paper are therefore consistent with the observations of A-segregates in ingot casting. The deffects could also nucleate freckles produced by the instability mentioned above. They could also cause freckles in a situation where isotherms are parallel if the deffect were to divert locally the flow parallel to isotherms in a direction normal to them.

5. CONCLUSSIONS

It has been shown that the main effect of gravity on interdendritic flow is to drive a flow parallel to the isotherms in a situations where the mushy zone is long and thin.

If the isotherms are not parallel, part of this flow is diverted in a directions normal to the isotherms. Simple approximate expressions have given for the magnitude of these diverted components. In all cases they attain maximum values at the liquidus, whose magnitude are strongly dependent on the assumptions made about the permeability near the liquidus. If the temperature fluctuates, then this diverted components are expected to produce freckles near the liquidus.

REFERENCES

1. Flemings, M.C. and Nereo, G.E.; Transactions of AIME vol 239 p. 1449, 1967.
2. Mehrabian, R., Keane, M. and Flemings, M.C.; Metallurgical Transaction vol. 1 p. 1209, 1970.
3. Piwonka, T.S. and Flemings, M.C.; Transaction of AIME, Transaction of AIME Vol. 236, p. 1157, 1966.
4. Kou, S., Poirier, D.R. and Flemings, M.C.; "Preceedings of Electric Furnace Conference, Chicage", Iron and Stcel Society of AIME, p. 221, 1977.
5. Jeanfils, C.L., Chen, J.H. and Klein, H.J.; AIME-TMS "Modelling of Casting and Welding Processes" edited by D. Apelian and H. Brody, 1981.
6. Favier, J.J.; Acta Metallurgia, Vol. 29 No 1 p. 197-205, 1981.
7. Kou, S.; Ph D. Thesis, MIT, Dept. of Mat. Science and Eng., 1979.
8. Rıdder, S.D., Kou, S. and Mehrabian, R.; "Met. Transaction vol. 12 B, p. 435, 1981.
9. Jeanfils, C.L. and Klein, H.J.; "Macrosegregation in a ESR melted Hastalloy Ingot". Conference paper, USA-USSR Joint Research Programme on Electrometallurgl, 1981.
10. Ohnaka, I. and Fukusako, T.; Transactions of ISN vol 21 p. 487, 1981.
11. Yerebakan, M.; Asymetric Permeability in a Freezing Sn-%20 Pb alloy, Special Report, NATO kod 0288, 1984.

APPENDIX 1. FLUID FLOW EOUATIONS

In this appendix, equations (4-6) will be obtained from (1-3). Equations (1-3) are expressed in a cartesian coordinate system. It is more convenient to change to an orthogonal system with the x_1 axis parallel to the isotherms and the fhird direction are assumed to be negligible. After this changes, equations (1-3) become;

$$\frac{\partial}{\partial t}(\rho_L g_L) - \rho_L \frac{\partial g_L}{\partial t} = -\frac{1}{l_1 l_2}\left[\frac{\partial}{\partial x_1}(l_1 \rho_L \xi_1) + \frac{\partial}{\partial x_2}(l_1 \rho_L \xi_2)\right] \quad (1.1)$$

$$\frac{\partial g_L}{\partial t} = -\left(\frac{1-\beta}{1-k}\right)\frac{\partial C_L/\partial T}{C_L}\left[g_L \frac{\partial T}{\partial t} + \frac{\xi_L}{l_2}\frac{\partial T}{\partial x_2}\right] \quad (1.2)$$

$$\xi_i = \frac{g_L K(g_L)}{\mu}\left[-\frac{1}{l_i}\frac{\partial p}{\partial x_i} + \rho_L \underset{\sim}{L}^i \underset{\sim}{g}\right] \quad (1.3)$$

The following new symbols have been introduced;

$$l_i = \left/ \frac{\partial \underset{\sim}{r}}{\partial k_i} \right/$$

$$L^i = \left(\frac{\partial r}{\partial k_i}\right) / l_i \qquad (i=1,2) \quad (1.4)$$

$$\xi_i = g_L V_i$$

Where $\underset{\sim}{r} = (x, y)$. The unknown p can be eleminated from the two equations (1.5) to give;

$$\frac{\partial}{\partial x_2}\left(\frac{l_1 \mu \xi_1}{g_L k}\right) - \frac{\partial}{\partial x_2}\left(\frac{l_2 \mu}{g_L k}\xi_2\right) = \frac{\partial}{\partial k_2}(l_1 \rho_L \underset{\sim}{L}' \underset{\sim}{g}) - \frac{\partial}{\partial x_2}(l_2 \rho_L \underset{\sim}{L}^2 \underset{\sim}{g})$$

which can be integrated with respect to x to give,

$$l_1 \mu \xi_1 = \int_{x_2(T_L)}^{x_2} dx_2 \left[\frac{\partial}{\partial x_1}\left(l_2 \frac{\mu}{\rho_L k}\xi_2 + l_1 \rho_L \underset{\sim}{L}^2 \underset{\sim}{g}\right)\right] + \left[l_1 \rho_L(x_2) \underset{\sim}{L}' \underset{\sim}{g} - l_1 \rho_L(x_2(T_L)) \underset{\sim}{L}^2 \underset{\sim}{g}\right] \quad (1.6)$$

In (1.6), T_L is the liquidus temperature, $x(T_L)$ is the liquidus position, which is independent of h because of the choice of coordinate axes. In obtaining equation 1-5, the usual boundry condition that the pressure at the liquidus is equal to $-\rho_L/g/y$ has been applied by using its consequence,

$$\xi_1(x_1(T_L)) = 0 \quad (11) \ ;$$

Equation 1,6 can be rewritten as;

$$l_1 \mu \xi_i = \int_{x_2(T_L)}^{x_2} dx \frac{\partial}{\partial x_1}\left(\frac{l_1 \mu \xi_2}{\rho_L k}\right) + A \quad (1.7)$$

Where the known function A is given by

$$A = [l_1 \rho_L (x_2) \underset{\sim}{L}' \underset{\sim}{g} - l_2 \rho_L (x_2 (T_L) \underset{\sim}{L}' \underset{\sim}{g}]$$

$$- \int_{x_2(T_L)}^{x_2} dx_2 \frac{\partial}{\partial x_1} (l_2 \rho_L \underset{\sim}{L} \underset{\sim}{g}) \qquad (1.8)$$

The new variables $\bar{\xi}_1$, and $\bar{\xi}_2$ defined as;

$$\bar{\xi}_1 = \xi_1 - g_L k A / l_1 \mu$$

$$\bar{\xi}_2 = \xi_2$$

are substituted into (1.1), (1.2) and (1.7) to give

$$\frac{\partial}{\partial t} (\rho_L g_L) - \rho_s \frac{\partial \rho_1}{\partial t} = - \frac{1}{l_1 l_2} \left[\frac{\partial}{\partial x_1} (\xi_1 l_2 \rho_L) + \frac{\partial}{\partial x_2} (\xi_2 l_1 \rho_L) \right] - B$$

$$\frac{\partial \rho_L}{\partial t} = - \left(\frac{1-\beta}{1-k} \right) \frac{\partial C_L / \partial t}{C_L} \left[\rho_L \frac{\partial T}{\partial t} + \frac{\xi_2 \partial T / \partial x_2}{l_2} \right] \quad . \quad . \quad . \quad . \qquad 1.10$$

$$\frac{l_1 \mu}{p_{2k}} \bar{\xi}_1 = \int_{x_2(T_L)}^{x_2} dx_2 \frac{\partial}{\partial x} \left(\frac{l_2 \mu \bar{\xi}_2}{g_L k} \right) \qquad 1.11$$

where

$$B = \frac{1}{l_1 l_2} \frac{\partial}{\partial x_1} [\rho_L k A l_2 \rho_L / l_1 \mu] \qquad 1.12$$

Finally V_p is set to be

$$V_{p_1} = kA / l_1 \mu$$

$$V_{p_2} = 0$$

and the steps leading to 1.8 - 1.10 are reversed to obtain equation (4-6).

APPENDIX 2. FLUID FOR NON-PARALLEL ISOTHERMS

In this appendix, a general expression for the gravity-driven component of the flow normal to isotherms is calculated. The isotherms are assumed to depart from being fiat and parallel by an amount characterised by a small parameter a.

Let 1_1^0, 1_2^0, $\bar{\xi}_1^0$, $\bar{\xi}_2^0$ and g_1 represent values of 1_1, 1_2, $\bar{\xi}_1$, $\bar{\xi}_2$, and respectively when a = 0, and let and represent the terms in these quantities linear in a. The initial coordinate system is chosen to set $1_1^0 = 1_2^0 = 1$ for convenience symbols have the same meanings as in Appendix 1.

To point out the size of the solidification shrinkage explicitly, a new small parameter is introduced:

$$\rho_s = \rho_{LL}(1+ \beta_o \phi_1(T))$$

$$\rho_L = \rho_{LL}(1+ \beta_o \phi_2(T))$$

where ρ_{LL} is the liquid density at the liquidus and ϕ_1 is chosen to ave value 1 at the liquidus temperature. In the case of the superalloy used in examples above, $\beta_0 = 0.053$.

After making these changes, the terms linear in a in (1,9 - 1,10) give

$$-\beta\left[\frac{\partial}{\partial t}(g_L'\phi_2)-\phi_1\frac{\partial g_L'}{\partial t}\right] = (1_1'+1_2')\frac{\partial}{\partial x_2}(\xi_2^o\rho_L)+\left[\frac{\partial}{\partial x_1}(\bar{\xi}_1\rho_L)\right.$$

$$\left.+\frac{\partial}{\partial x_2}(\bar{\xi}_2\rho_L)\right]+B \qquad 2.1$$

$$g_L' = \int_{t_L}^{t} dt'\{[\bar{\xi}_2'\, 1_2'\, \bar{\xi}_2^o]\,\lambda\frac{\partial T}{\partial x_2}\, I(t')\} / I(t) \qquad 2.2$$

$$\frac{u\,\bar{\xi}_1'}{g_L k} = \int_{x_2(T_L)}^{x_2} dx_2\, a\frac{\partial}{\partial a}\left(\frac{\partial}{\partial x_1}\left(\frac{1_2 u\,\bar{\xi}_2}{g_L k}\right)\right) \qquad 2.3$$

where I (t) and λ are defined by

$$I(t) = \exp\left(\int_o^t dt\lambda\ \partial T/\partial t\right)$$

$$\lambda = \left(\frac{1-\beta}{1-k}\right)\partial C_L / \partial T$$

and is the time when the temperature decreased below the liquidus. The fact that $\bar{\xi}_1^0 = 0$ has been used in obtaining (1.1) and (1.3).

In the cases of interest. $1'_1$, $1'_2$ and B depend on x linearly. We seek a solution of (2.1-2.3) in which $\bar{\xi}'_1$, $\bar{\xi}'_2$ and g'_L have a similar dependence on x,. In this case, from (2.3), $\bar{\xi}'_1$ is independent of x, which in turn implies that the term

in (2.1) is zero. (2.1) and (2.2) then constitute a set of coupled equations involving the unknowns $\overline{\xi'}_2$ and g'_L only.

Now, the approximation that β_0 is small is introduced. From (1.7), B is proportional to β_0, as is $\overline{\xi}^0_2$. Thus, from (2.1), is proportional to β_0 and so, from (2.2), g'_L is proportional to β_0. Thus, in (2.1), the left side is propertional to β_0^2 and will consequently be ignored. Hence (2.1) simplifies to

$$\frac{\partial}{\partial x_2} \left(\overline{\xi}'_2 \rho_L \right) + (1'_1 + 1'_2) \frac{\partial}{\partial x_2} \left(\overline{\xi}^0_2 \rho_L \right) + B = 0 \qquad (2.4)$$

which has the solution

$$\overline{\xi}'_2 = \frac{-1}{\rho_L} \int_{x_2(T_E)}^{x_2} dx_2 \left[B + (1'_1 + 1'_2) \frac{\partial}{\partial x_2} \left(\overline{\xi}^0_2 \rho_L \right) \right] \qquad (2.5)$$

where T_E is the eutectic temperature. The component $\overline{\xi}'_{2g}$ of induced by gravity is therefore given by

$$\overline{\xi}'_{2g} = \frac{-1}{\rho_L} \int_{x_2(T_E)}^{x_2} dx_2 \; B \qquad (2.6)$$

Finally, from (1.11)

$$V_{2g} = \frac{-1}{g_L \rho_L} \int_{x_2(T_E)}^{x_2} dx_2 \; \nabla (\rho_L g_L V_p) \qquad (2.7)$$

APPENDIX 3. FLUID FLOW IN SOME SPECIAL CASES

We now specialise to particular isotherm geometries. In the system with isotherms parallel to the surfaces

$$y - ax^2 = \text{constant} \tag{3.1}$$

the new coordinates x_1, x_2 defined by

$$\begin{aligned} x_1 &= x\,(1+2ay) \\ x_2 &= y - ax^2 \end{aligned} \tag{3.2}$$

constitute an orthogonal system to first order in a. 1_1 and 1_2 are then 1-2 ay and 1 respectively to first order in a. From these and (1.8), A is

$$\frac{g_L k}{\mu}\left[\{\rho_L(x_2)\,[g_1 + 2ax_1 g_2] - \rho_L(x_2(T_L))\,[g_1 + 2ax_1 g_2]\} - \int_{x_2(T_L)}^{x_2} dx_2\, 2a\rho_L\, g_1\right] \tag{3.3}$$

and hence

$$\overline{\xi}'_{2g} = -2ag_2\,\tau(x_2) \tag{3.4}$$

where

$$J = \frac{1}{\rho_L}\int_{x_2(T_E)}^{x_2} \rho_L \frac{F}{\mu}\left(\rho_L(x_2) - \rho_L(x_2(T_L))\right) d x_2 \tag{3.4}$$

Similarly, for thne system with isotherms parallel to the sur faces

$$y\,(1+2ax) = \text{constant} \tag{3.5}$$

the coordinates x_1, x_2 defined by

$$\begin{aligned} x_1 &= x - ay^2 \\ x_2 &= y\,(1+2ax) \end{aligned} \tag{3.6}$$

are orthogonal and the value of A is

$$\frac{g_L k}{\mu}\left[\{\rho_L(x_2)(g_1 - 2ax_2 g_L) - \rho_L(x_2(T_L))(g_1 - 2ax_2(T_L))\, g_2\} - \int_{x_2(T_L)}^{x_2} dx_2\, 2a\rho_L g_1\right] \tag{3.7}$$

From this,

$$\overline{\xi}'_{2g} = 2ag_1 J(x_2) \tag{3.8}$$

The final case of interest occurs when a circular ingot is considered. In this case, (1) is replaced by

$$\frac{\partial}{\partial t}(\rho_L g_L) - \rho_s \frac{\partial g}{\partial t} = -\left[\frac{\partial}{\partial r}(\partial_L \xi_r) + \frac{\partial}{\partial z}(\rho_L \xi_z)\right] - \frac{\rho_L \xi_r}{r} \tag{3.9}$$

The arguments leading to (B4) remain essentially unchanged, except that the term $-\rho_L \xi r / r$ needs to be retainde on the right gide in place of B and that

$$\frac{\partial}{\partial x_2}(\overline{\xi}'_2 \rho_L) + \frac{\overline{\xi}^0_2 \rho_L \sin\theta}{r} + \frac{\overline{\xi}^0_1 \rho_L \cos\theta}{r} = 0 \tag{3.10}$$

where is the angle between the isotherm normal and the vertical. The component ξ'_{2g} of ξ'_2 due to gravity and the curvature of the mold is then

$$-\frac{g_1 \cos\theta}{r} J(x_2) \tag{3.11}$$